

## Modeling Ekman and quasi-static magnetohydrodynamic turbulence using Pao's hypothesis

Mohammad Anas <sup>\*</sup>

*Department of Mechanical Engineering, Indian Institute of Technology, Kanpur 208016, India*

Mahendra K. Verma <sup>†</sup>

*Department of Physics, Indian Institute of Technology, Kanpur 208016, India*



(Received 10 July 2019; published 28 October 2019)

Two-dimensional (2D) turbulence with Ekman friction and quasi-static magnetohydrodynamic (QS MHD) turbulence are complex flows. In this paper, we present models for these flows by extending Pao's hypothesis [Phys. Fluids 8, 1063 (1965)] for hydrodynamic turbulence to them. For 2D Ekman turbulence, the energy spectrum predicted by the model is steeper than its hydrodynamic counterpart due to Ekman friction. The model predictions are consistent with earlier theoretical predictions and experimental and numerical results. Similarly, the model for QS MHD turbulence predicts a steeper energy spectrum due to Joule dissipation; the model predictions fit with earlier numerical results quite well.

DOI: [10.1103/PhysRevFluids.4.104611](https://doi.org/10.1103/PhysRevFluids.4.104611)

### I. INTRODUCTION

To date, turbulence remains a poorly understood phenomenon. One of the important known results of three-dimensional (3D) turbulence is due to Kolmogorov [1,2], according to which a constant energy flux cascades from large scales to small scales, leading to energy-spectrum scaling as

$$E_u(k) = K_{K_0} \epsilon_u^{2/3} k^{-5/3}. \quad (1)$$

Here,  $\epsilon_u$  is the energy flux, and  $K_{K_0}$  is Kolmogorov's constant. The above energy spectrum and flux have been observed in three-dimensional homogeneous isotropic turbulence at high Reynolds number [3–6] but is modified for different forcing. For example, inclusion of rotation, magnetic field, and buoyancy alter turbulence properties significantly [5,7–11]. In some flows, the presence of an external dissipation (for example, Ekman friction [12–14] and Joule dissipation [10,15]) dampens the energy of multiscale flow structures more than that predicted by Kolmogorov's theory. This leads to steepening in the energy flux and spectrum. Modeling such complex flows is quite difficult. Fortunately, an extension of Pao's hypothesis for hydrodynamic turbulence offers a set of models for two-dimensional (2D) Ekman turbulence and quasi-static magnetohydrodynamic (QS MHD) turbulence; this is the topic of the present paper.

Friction at the bottom of the container in a shallow layer [16], and the friction of the surrounding air in soap film [17] induce drag which is commonly termed *Ekman friction*. Such flows are typically modeled as 2D turbulence because of the shallow nature of the flow, and they have been widely studied by researchers using experiments and numerical simulations. A common theme in

<sup>\*</sup>anas@iitk.ac.in

<sup>†</sup>mkv@iitk.ac.in

these works is that the Ekman friction yields a steeper energy spectrum than that predicted by Kraichnan [18] in the forward enstrophy cascade regime; that is,  $E_u(k) \sim k^{-3-\xi}$  where  $\xi$  is the correction in the spectral exponent.

Belmonte *et al.* [19] performed an experiment on soap film and observed  $E_u(k) \sim k^{-3.3}$ . In a similar experiment of soap film freely suspended by an electromagnetic force, Rivera and Wu [20] reported a significant energy dissipation due to atmospheric drag. Boffetta *et al.* [21] performed an experiment on a thin layer of fluid flow driven by electromagnetic force and observed a steeper energy spectrum due to the bottom friction. They predicted an energy spectrum as  $E_u(k) \sim k^{-3-2\alpha/\lambda}$ , where  $\lambda$  is the Lyapunov exponent of the vorticity field ( $\boldsymbol{\omega} = \nabla \times \mathbf{u}$ ) and  $\alpha$  is the coefficient of Ekman friction. They assumed that  $\lambda \propto \omega_{\text{rms}}$ , where  $\omega_{\text{rms}}$  is the root mean square vorticity, which can be calculated by using the velocity field. Refer to reviews [22,23] for additional works in this field.

Boffetta *et al.* [24] performed numerical simulations of 2D Ekman turbulence with enstrophy injections at large scales and reported a steeper energy spectrum compared with Kraichnan's theory of 2D turbulence. Nam *et al.* [12] also observed similar results, and derived a complex expression for  $\xi$  in terms of the frictional coefficient  $\alpha$  and probability distribution function for a finite-time Lyapunov exponent. Using variable enstrophy flux theory, Verma [13] assumed the enstrophy flux to be variable in wave number and derived formulas for the enstrophy flux and spectrum in the inertial-dissipation range. Verma's formulas provide a good fit to the inertial-range spectrum.

Liquid metal flows are observed in planetary cores and many engineering applications [25,26]. Note that liquid metals have very low magnetic Prandtl number  $\text{Pm}$ , which is the ratio of kinematic viscosity  $\nu$  to magnetic diffusivity  $\eta$  of the fluid. A special class of MHD flows is quasi-static magnetohydrodynamics (QS MHD) for which the magnetic Reynolds number  $\text{Rm} = U_0 L / \eta \ll 1$  [10,27]; here,  $U_0$  and  $L$  are the large-scale velocity and length, respectively. For this case, the energy is dissipated both by the Joule dissipation and viscous dissipation.

The effect of Joule dissipation in QS MHD turbulence has been studied by many researchers. Because of Joule dissipation, energy flux is no longer constant, and the energy spectrum becomes steeper than the corresponding hydrodynamic energy spectrum [28]. The steepening of the spectrum depends on the intensity of the applied magnetic field, or the interaction parameter  $N$ , which is the ratio of the Lorentz force to the nonlinear term. Using numerical simulations, Hossain [29] observed that, for  $N = 10$ ,  $E_u(k) \sim k^{-3}$ , similar to that found in 2D turbulence [18]. Using the perturbative method, Ishida [30] derived that  $E_u(k) \sim k^{-7/3}$ ; in the same work, they obtained a similar energy spectrum by using a numerical simulation. Vorobev *et al.* [31] performed direct numerical simulation (DNS) and large eddy simulations (LESs) for  $N = 0$  to 5 and observed that the spectrum becomes steeper and steeper (from  $k^{-5/3}$  to  $k^{-3}$ ) with increasing  $N$ .

Verma and Reddy [28] derived analytic expressions for the energy spectrum and flux by postulating a  $k$ -dependent  $\Pi_u(k)$  in the inertial-dissipation range, and substituting it in place of the dissipation rate in Pope's model [3] for the energy spectrum. Their model captures the energy flux and spectrum in the inertial range quite well, but there is a significant discrepancy between the model predictions and the numerical results in the dissipation range. This deficiency induced us to explore an extension of Pao's model of hydrodynamic turbulence to QS MHD turbulence.

Before the construction of new models for Ekman and QS MHD turbulence, it is best to summarize Pao's model for hydrodynamic turbulence. To extend Kolmogorov's spectrum in the inertial range to the dissipation range, Pao [32] conjectured that, for three-dimensional homogeneous isotropic turbulence,  $E_u(k)/\Pi_u(k)$  is independent of viscosity, and it depends solely on the total energy dissipation rate  $\epsilon_u$  and wave number  $k$ , where  $\Pi_u(k)$  is the energy flux. Hence, using dimensional analysis, we get

$$\frac{E_u(k)}{\Pi_u(k)} = K_{\text{Ko}} \epsilon_u^{-1/3} k^{-5/3}. \quad (2)$$

Substituting this into the equation for variable energy flux,  $d\Pi_u(k)/dk = -2\nu k^2 E_u(k)$ , yields

$$E_u(k) = K_{\text{Ko}} \epsilon_u^{2/3} k^{-5/3} \exp \left[ -\frac{3}{2} K_{\text{Ko}} \left( \frac{k}{k_d} \right)^{4/3} \right], \quad (3)$$

where  $k_d = (\epsilon_u/\nu^3)^{1/4}$  is the Kolmogorov wave number. Recently, Verma *et al.* [33] verified Pao's model by using direct numerical simulation. In the present paper, we extend Pao's hypothesis to model the energy spectrum of 2D Ekman turbulence and QS MHD turbulence.

The paper is organized as follows: In Sec. II, we review the role of Ekman friction in 2D turbulence, develop a model for the steeper energy spectrum, and compare our predictions with earlier results. In Sec. III, we perform similar analysis for QS MHD turbulence with  $N \lesssim 1$ . We conclude in Sec. IV.

## II. MODELING TWO-DIMENSIONAL TURBULENCE WITH EKMAN FRICTION

In this section, we employ Pao's hypothesis to derive energy spectrum and flux for the inertial-dissipation range of 2D Ekman turbulence. We show how Ekman friction is responsible for the steeper energy spectrum in 2D turbulence. We also compare the model predictions with earlier experimental and numerical results.

### A. Derivation of energy spectrum for Ekman turbulence using Pao's hypothesis

The governing equations for the vorticity field of a 2D ( $xy$  plane) flow with Ekman friction are

$$\frac{\partial \omega}{\partial t} + (\mathbf{u} \cdot \nabla) \omega = -\alpha \omega + \nu \nabla^2 \omega + f_\omega, \quad (4)$$

$$\nabla \cdot \mathbf{u} = 0, \quad (5)$$

where  $\mathbf{u}$  is the velocity field,  $\omega = (\nabla \times \mathbf{u}) \cdot \hat{z}$  is the vorticity field, and  $f_\omega = (\nabla \times \mathbf{f}_u) \cdot \hat{z}$ , with  $\mathbf{f}_u$  being the external acceleration (apart from Ekman friction). The Ekman friction is modeled as  $-\alpha \mathbf{u}$ , where  $\alpha$  is the linear frictional coefficient. Equation (5) follows due to the incompressibility condition.

We assume that the flow is forced at  $k_f \approx 1/L$ , where  $L$  is the system size. Under this forcing, for the pure hydrodynamic case ( $\alpha = 0$ ), in the inertial range we expect a constant enstrophy flux and  $k^{-3}$  energy spectrum [18]:

$$E_u(k) = K_{2D} \epsilon_\omega^{2/3} k^{-3}, \quad (6)$$

$$\Pi_\omega(k) = \epsilon_\omega, \quad (7)$$

where  $K_{2D}$  is a constant, and  $\epsilon_\omega$  is the total enstrophy dissipation rate. Note that  $E_\omega(k) = k^2 E_u(k) \sim k^{-1}$ . Also, the flow does not exhibit inverse energy cascade due to absence of the  $k < k_f$  regime. In the present paper we extend the above inertial spectrum to the inertial-dissipation range for nonzero  $\alpha$ .

The evolution equation for the one-dimensional enstrophy spectrum is [13]

$$\frac{\partial}{\partial t} E_\omega(k, t) = -\frac{\partial}{\partial k} \Pi_\omega(k, t) - (2\nu k^2 + 2\alpha) E_\omega(k, t) + \mathcal{F}_\omega(k, t). \quad (8)$$

Here, the terms  $2\nu k^2 E_\omega(k)$  and  $2\alpha E_\omega(k)$  represent the rate of enstrophy dissipation due to viscosity and Ekman friction, respectively, and  $\mathcal{F}_\omega(k)$  is the enstrophy injection rate by the external force. In the steady state,  $\partial E_\omega(k, t)/\partial t = 0$ , in the inertial-dissipation range where  $\mathcal{F}_\omega(k) = 0$ , Eq. (8) gets transformed to

$$\frac{d}{dk} \Pi_\omega(k) = -2(\nu k^2 + \alpha) E_\omega(k). \quad (9)$$

The above equation indicates that the viscous friction is significant in the dissipation range (large  $k$ ). However, Ekman friction is significant at all values of  $k$  and hence suppresses the enstrophy flux in the inertial range itself. To solve Eq. (9), we extend Pao's model for 3D hydrodynamic turbulence to such flows as follows: We assume that  $E_\omega(k)/\Pi_\omega(k)$  depends solely on  $\epsilon_\omega$  and  $k$ , but not on  $\nu$  or the forcing function. Therefore, dimensional analysis yields

$$\frac{E_\omega(k)}{\Pi_\omega(k)} = K_{2D}\epsilon_\omega^{-1/3}k^{-1}. \quad (10)$$

Substitution of  $E_\omega(k)$  of Eq. (10) into Eq. (9) and an integration yields

$$\Pi_\omega(k) = \Pi_\omega(k_0) \left(\frac{k}{k_0}\right)^{-2\alpha K_{2D}\epsilon_\omega^{-1/3}} \exp\left[-\frac{K_{2D}}{k_{d2D}^2}(k^2 - k_0^2)\right], \quad (11)$$

where  $\Pi_\omega(k_0)$  is the reference enstrophy flux corresponding to  $k = k_0$ , and  $k_{d2D} = (\epsilon_\omega^{1/3}/\nu)^{1/2}$ . We choose  $k_0$  where enstrophy flux is a maximum, and hence  $\Pi_\omega(k_0) = \epsilon_\omega$ . Substitution of  $\Pi_\omega(k)$  from Eq. (11) into Eq. (10) and using  $\Pi_\omega(k_0) = \epsilon_\omega$  and  $E_u(k) = k^{-2}E_\omega(k)$ , we obtain

$$E_u(k) = K_{2D}\epsilon_\omega^{2/3}k^{-3} \left(\frac{k}{k_0}\right)^{-2\alpha K_{2D}\epsilon_\omega^{-1/3}} \exp\left[-\frac{K_{2D}}{k_{d2D}^2}(k^2 - k_0^2)\right]. \quad (12)$$

Thus, we derive the enstrophy flux and energy spectrum for Ekman turbulence by using Pao's hypothesis. Clearly, both quantities, enstrophy flux and spectrum, steepen relative to those of 2D turbulence. The correction in the spectral exponent of the energy spectrum due to Ekman friction is

$$\xi_m = -2\alpha K_{2D}\epsilon_\omega^{-1/3}. \quad (13)$$

Here the subscript "m" stands for the model. The above prediction of  $\xi_m \propto \alpha$  is consistent with the results of Nam *et al.* [12]. In addition, Boffetta *et al.* [21] predict the correction to be  $2\alpha/\lambda$ , where  $\lambda$  is the Lyapunov exponent for the evolution of the vorticity fluctuations. Also,

$$\lambda = \omega_{\text{rms}} \propto \frac{1}{\epsilon_\omega^{1/3}}. \quad (14)$$

Hence, the prediction of Boffetta *et al.* [21] for the correction in the spectral exponent has a similar form as that of Eq. (13).

In the next section, we compare the model predictions with earlier experimental and numerical results.

## B. Comparison of model predictions with earlier results

We compare the aforementioned model predictions for the spectrum and flux with earlier experiments of Boffetta *et al.* [21] and the simulation of Boffetta *et al.* [24]. Boffetta *et al.* [21] performed experiments on a thin layer of an electromagnetically driven fluid—an electrolyte solution of water and sodium chloride—for  $\alpha = 0.037, 0.059$ , and  $0.069$  and obtained the corresponding corrections in the spectral exponent  $\xi$ . In addition, Boffetta *et al.* [24] performed a direct numerical simulation with forcing at large scales and the enstrophy injection rate maintained at  $\epsilon_\omega = 0.16$ . They reported that, for  $\alpha = 0.15$ , the energy spectrum is steeper than that of 2D hydrodynamic turbulence, with the correction being  $\xi \approx 1.20$ .

In Table I we list the spectral corrections reported in the experiments of Boffetta *et al.* [21], and the DNS of Boffetta *et al.* [24], along with the corresponding predictions by the model [Eq. (13)]. We estimate  $\epsilon_\omega$  for the experimental data by using

$$\epsilon_\omega = \int_0^\infty 2\nu k^4 E_u(k) dk,$$

TABLE I. For 2D Ekman turbulence, this table lists the spectral corrections by model predictions ( $\xi_m = 2\alpha K_{2D}\epsilon_\omega^{-1/3}$ ) and experimental and numerical results.  $\alpha = 0.037, 0.059$ , and  $0.069$  correspond to Ref. [21], and  $\alpha = 0.15$  belongs to Ref. [24]. We obtain  $K_{2D} = 1.6 \pm 0.3$  for the experimental case from the compensated energy spectra and assume  $K_{2D} = 2.2 \pm 0.3$  for the DNS case. The errors in  $\xi_m$  are computed by using the uncertainties in the constant  $K_{2D}$ .

$\alpha$ ( $s^{-1}$ )	$\epsilon_\omega$ ( $s^{-3}$ )	$\xi$	$\xi_m$
0.037	$2.0 \times 10^{-2}$	$0.50 \pm 0.01$	$0.44 \pm 0.09$
0.059	$1.0 \times 10^{-2}$	$0.80 \pm 0.02$	$0.87 \pm 0.17$
0.069	$9.4 \times 10^{-3}$	$1.00 \pm 0.02$	$1.05 \pm 0.21$
0.15	$1.6 \times 10^{-1}$	$1.2 \pm 0.2$	$1.2 \pm 0.2$

where  $\nu = 0.01$  cm<sup>2</sup>/s for the electrolyte, which is mostly water. The constant  $K_{2D}$  is reported to vary between 1.3 to 1.7 for 2D turbulence [23]. Since we do not have data for  $\alpha = 0$ , we compute  $K_{2D}$  for the lowest  $\alpha$  (0.037) by using the compensated energy spectrum [ $K_{2D} = k^3 E_u(k) \epsilon_\omega^{-2/3}$ ]. As illustrated in Fig. 1(a),  $K_{2D} = 1.6 \pm 0.3$ . As shown in Table I, the estimated  $\xi_m$  using experimental data varies from 0.44 to 1.05 and matches quite closely the experimental results.

In Fig. 2 we illustrate the energy spectra reported in the experiments of Boffetta *et al.* [21] and the model predictions [Eq. (12)] for  $\alpha = 0.037, 0.059$ , and  $0.069$ . It is evident that the energy spectra are steeper than Kraichnan's prediction [ $E_u(k) \sim k^{-3}$ ]. The predicted spectra by the model fit well with the experimental results in the inertial range. Each of the functions  $E_u(k)$  from Boffetta *et al.* [21] exhibit a slight bump near the transition zone from the inertial range to the dissipation range. This feature appears similar to the bottleneck effect, which has been primarily observed in 3D hydrodynamic turbulence [34–36], and in magnetohydrodynamic turbulence [37]. However, the bottleneck effect in 2D hydrodynamic turbulence needs to be studied in detail in the future.

Similarly, in Fig. 3, we exhibit the enstrophy spectrum and flux obtained from the DNS of Boffetta *et al.* [24] and the predictions of our model. In this case, the energy spectrum,  $E_u(k) \sim k^{-4.2}$ , is significantly steeper than  $E_u(k) \sim k^{-3}$  in the inertial range, so we cannot get a constant value of  $K_{2D}$  in the power-law regime by using the compensated energy spectra. Here, we had to employ  $K_{2D} = 2.2 \pm 0.3$  in Eq. (12) to get a better agreement with the numerical results. With this caveat, the model predictions and numerical results are quite close to each in the inertial range, but they differ in the dissipation range. As shown in Fig. 3, our model [Eqs. (11) and (12)] underpredicts the energy flux and spectrum in the dissipation range. To compensate for this deficiency, we modify the kinematic viscosity as  $\nu \rightarrow c\nu$ , where  $c$  is a constant. We observe the best fit to the numerical results for  $c = 0.2$ . See Fig. 3 for an illustration.

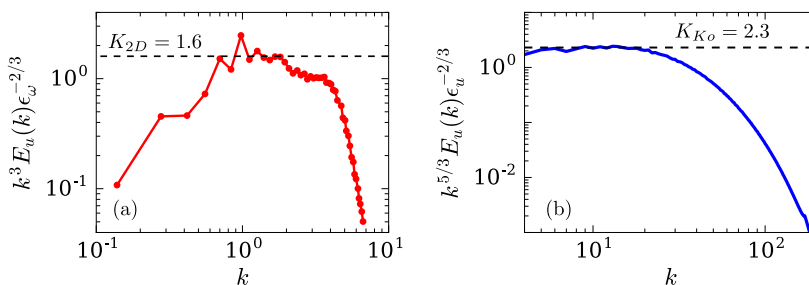


FIG. 1. Computation of  $K_{2D}$  and  $K_{K_0}$  for 2D Ekman and QS MHD turbulence, respectively, using the compensated energy spectrum. (a)  $K_{2D} = 1.6$  for 2D Ekman turbulence using the experimental data of Boffetta *et al.* [21] for  $\alpha = 0.037$ . (b)  $K_{K_0} = 2.3$  computed by using the  $N = 0$  numerical run of Verma and Reddy [28].

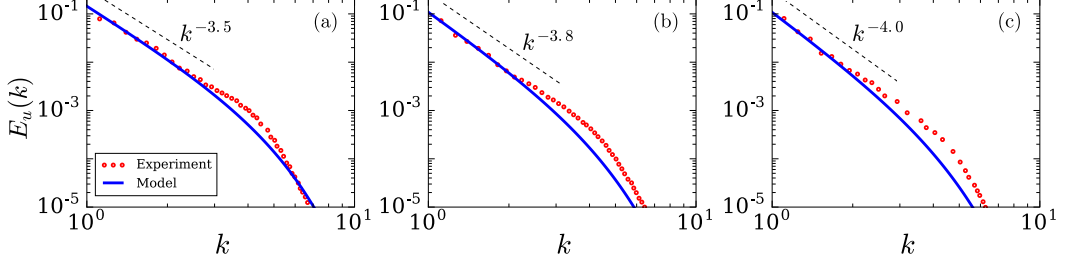


FIG. 2. 2D Ekman turbulence: Plots of energy spectrum reported in the experiments of Boffetta *et al.* [21] (circles), and the model predictions of Eq. (12) (solid lines) for (a)  $\alpha = 0.037$ , (b)  $\alpha = 0.059$ , and (c)  $\alpha = 0.069$ . The dashed lines represent fits in the inertial range.

Thus, we demonstrate that our model of Ekman turbulence based on Pao's hypothesis provides a good fit to the past experimental and numerical results of Ekman turbulence. In the next section, we construct a similar model for QS MHD turbulence.

### III. MODELING QUASI-STATIC MAGNETOHYDRODYNAMIC TURBULENCE

In this section, we develop a model for the energy spectrum of QS MHD turbulence by using Pao's hypothesis. We compare predictions of our model with earlier numerical results.

#### A. Basic equations and model based on Pao's hypothesis

The nondimensional form of the governing equations for liquid metal flows with  $\text{Rm} \approx 0$  (the quasi-static approximation) are [10,25,26]

$$\frac{\partial \mathbf{u}}{\partial t} + (\mathbf{u} \cdot \nabla) \mathbf{u} = -\nabla p - \frac{L}{\eta U_0} \Delta^{-1} [(\mathbf{B}_0 \cdot \nabla)^2 \mathbf{u}] + \frac{1}{\text{Re}} \nabla^2 \mathbf{u} + \mathbf{f}, \quad (15)$$

$$\nabla \cdot \mathbf{u} = 0, \quad (16)$$

where  $\Delta^{-1}$  is the inverse of the Laplacian operator,  $\mathbf{u}$  is the velocity field,  $p$  is the pressure field,  $\mathbf{B}_0 = B_0 \hat{z}$  is the mean magnetic field in velocity units, Reynolds number  $\text{Re} = U_0 L / \nu$ , and  $\mathbf{f}$  is the external force field. The corresponding momentum equation in Fourier space is [10,27]

$$\frac{\partial \hat{u}_i(\mathbf{k})}{\partial t} = -ik_i \hat{p}(\mathbf{k}) - ik_j \sum_{\mathbf{q}} \hat{u}_j(\mathbf{q}) \hat{u}_i(\mathbf{k} - \mathbf{q}) - \frac{B_0^2 L}{U_0 \eta} (\cos^2 \zeta) \hat{u}_i(\mathbf{k}) - \frac{1}{\text{Re}} k^2 \hat{u}_i(\mathbf{k}) + \hat{f}_i(\mathbf{k}), \quad (17)$$

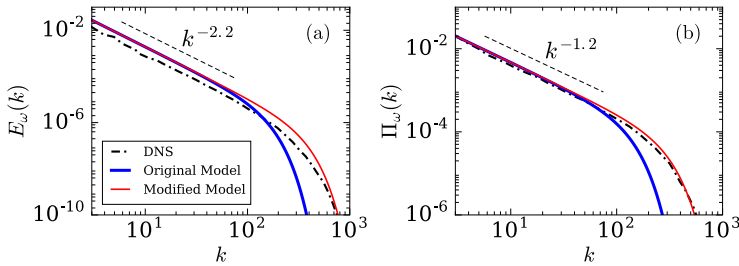


FIG. 3. 2D Ekman turbulence: The predictions of the model [Eqs. (11) and (12)], match with the plots of Boffetta *et al.* [24] of (a) the entrophy spectrum and (b) entrophy flux (dot-dashed black lines) for  $\alpha = 0.15$ . The model plots are for the original model with  $\nu$  from DNS (thick solid blue lines) and for the modified model with  $0.2\nu$  (thin solid red lines).

where  $\hat{u}(\mathbf{k})$  is the Fourier transform of the velocity field, and  $\zeta$  is the angle between  $\mathbf{B}_0$  and wave number  $\mathbf{k}$ . In the above equation,

$$N = \frac{B_0^2 L}{U_0 \eta}, \quad (18)$$

which is called the interaction parameter, represents the ratio of the Lorentz force to the nonlinear term. The evolution equation for the one-dimensional energy spectrum is [10,28]

$$\frac{\partial}{\partial t} E_u(k, t) = -\frac{\partial}{\partial k} \Pi_u(k, t) - 2\nu k^2 E_u(k, t) - 2N c_2 E_u(k, t) + \mathcal{F}_u(k), \quad (19)$$

where

$$c_2 = \int_0^\pi \cos^2 \zeta \frac{g(\zeta)}{\pi} d\zeta. \quad (20)$$

Here,  $g(\zeta)$  describes the angular dependence of the energy spectrum due to anisotropy,  $\Pi_u(k)$  is the energy flux,  $2\nu k^2 E_u(k)$  is the viscous dissipation rate,  $2N c_2 E_u(k)$  is the Joule dissipation rate, and  $\mathcal{F}_u(k)$  is the energy injection rate by the external force.

The behavior of the energy spectrum in QS MHD depends crucially on  $N$ . For  $N \rightarrow 0$ , Joule dissipation becomes negligible, and we observe the properties of QS MHD to be similar to those of hydrodynamic turbulence. However, for  $N \lesssim 1$ , Joule dissipation becomes significant, and it results in a considerable decrease in the energy flux in the inertial range. Consequently, the energy spectrum becomes steeper. This steepening of the energy spectrum due to Joule dissipation is reported in various experiments [38,39] and numerical simulations [15,31,40,41]. At moderately large  $N$ , the flow becomes quasi-two-dimensional. For this range, Hossain [29] and Alemany *et al.* [38] argued that  $E_u(k) \sim k^{-3}$ , but others have argued that the spectral index will vary with  $N$  [10,15,40]. In case of very high  $N$  ( $> 100$ ), Joule dissipation becomes so strong that the energy spectrum becomes exponential with  $E_u(k) \sim \exp(-bk)$  [42], where  $b$  is a constant. In this study, we consider the regime  $N \lesssim 1$  only and analyze the steepening of the energy spectrum and flux by using Pao's hypothesis. This is because the energy spectrum for this case is closer to that described by Kolmogorov's theory and Pao's model. For larger  $N$ , we need to model complex quasi-2D turbulence.

For a steady state and in the inertial-dissipation range where  $\mathcal{F}_u(k) = 0$ , Eq. (19) becomes

$$\frac{d}{dk} \Pi_u(k) = -(2\nu k^2 + 2N c_2) E_u(k). \quad (21)$$

At high Reynolds number and  $N \lesssim 1$ , we can expect Pao's hypothesis (2) to perform well. Substitution of  $E_u(k)$  from Eq. (2) into Eq. (21) and integrating yields

$$\Pi_u(k) = \Pi_u(k_0) \exp \left\{ -\frac{3}{2} K_{\text{Ko}} \left[ \left( \frac{k}{k_d} \right)^{4/3} - \left( \frac{k_0}{k_d} \right)^{4/3} \right] + 3c_2 K_{\text{Ko}} \left[ \left( \frac{k}{k_{d2}} \right)^{-2/3} - \left( \frac{k_0}{k_{d2}} \right)^{-2/3} \right] \right\}. \quad (22)$$

Here,  $\Pi(k_0) \approx \epsilon_u$  is the reference energy flux at wave number  $k_0$ ,  $k_d = (\epsilon_u/\nu^3)^{1/4}$ , and  $k_{d2} = (N^3/\epsilon_u)^{1/2}$ . Note that  $\Pi(k)$  decreases from  $\Pi(k_0)$  with the increase of  $k$ . Substitution of the above  $\Pi_u(k)$  into Eq. (2) provides the energy spectrum:

$$E_u(k) = K_{\text{Ko}} \epsilon_u^{2/3} k^{-5/3} \exp \left\{ -\frac{3}{2} K_{\text{Ko}} \left[ \left( \frac{k}{k_d} \right)^{4/3} - \left( \frac{k_0}{k_d} \right)^{4/3} \right] + 3c_2 K_{\text{Ko}} \left[ \left( \frac{k}{k_{d2}} \right)^{-2/3} - \left( \frac{k_0}{k_{d2}} \right)^{-2/3} \right] \right\}. \quad (23)$$

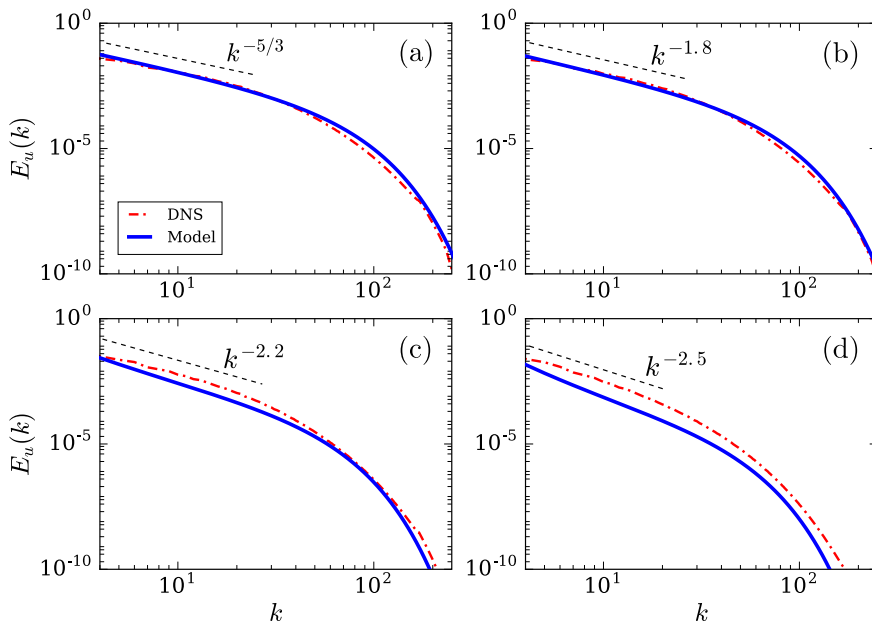


FIG. 4. For QS MHD turbulence, plots of the energy spectrum for (a)  $N = 0.0$ , (b)  $N = 0.1$ , (c)  $N = 0.5$ , and (d)  $N = 1.0$  reported in the numerical simulations of Ref. [28] (dot-dashed lines) and by model prediction (solid lines).

Thus we derive the energy flux and spectrum for quasi-static MHD turbulence for small  $N$  by using Pao's hypothesis. In these expressions, the second term in the exponential yields more steepening than the hydrodynamic counterpart due to Joule dissipation. Equation (23) is also valid for pure hydrodynamic turbulence; we recover Pao's model [Eq. (3)] for  $N = 0$ .

In the next section, we compare the prediction of the model with earlier numerical results.

### B. Comparison of prediction of the model with earlier numerical results

To verify the effectiveness of the model discussed in the previous section, we compare the model predictions with the numerical results of Verma and Reddy [28]. Verma and Reddy [28] simulated QS MHD turbulence for a wide range of  $N$  and demonstrated steepening of the energy spectrum compared with hydrodynamic turbulence. In this section, we focus on the  $N \lesssim 1$  regime because our model is applicable to this range of  $N$ .

For a comparison of model predictions and numerical results, we consider  $N = 0.0, 0.1, 0.5$ , and  $1.0$ . The Kolmogorov constant  $K_{K_0}$  is computed by using the compensated energy spectrum [Fig. 1(b)] for  $N = 0$ . Although the computed value,  $K_{K_0} \approx 2.3$ , is slightly larger than that proposed value ( $K_{K_0} \approx 1.6$ ) for high-Reynolds-number turbulence [43,44], this difference is frequently observed in DNS at moderate Reynolds number [33]. In Figs. 4 and 5, we exhibit the energy spectrum and flux obtained from the DNS and those predicted by the model [Eqs. (23) and (22)]. We observe that the energy spectrum and flux become steeper with increasing  $N$ . The predicted energy spectra and fluxes fit well with the numerical results in both the inertial and dissipation ranges.

Earlier, Verma and Reddy [28] constructed a similar model as above, but with Pope's prescription [3] for the energy spectrum. The model of Verma and Reddy [28] describes the inertial range well, but it falters for the dissipation range. In comparison, the present model based on Pao's prescription describes both the inertial and dissipation ranges quite well.

We conclude in the next section.

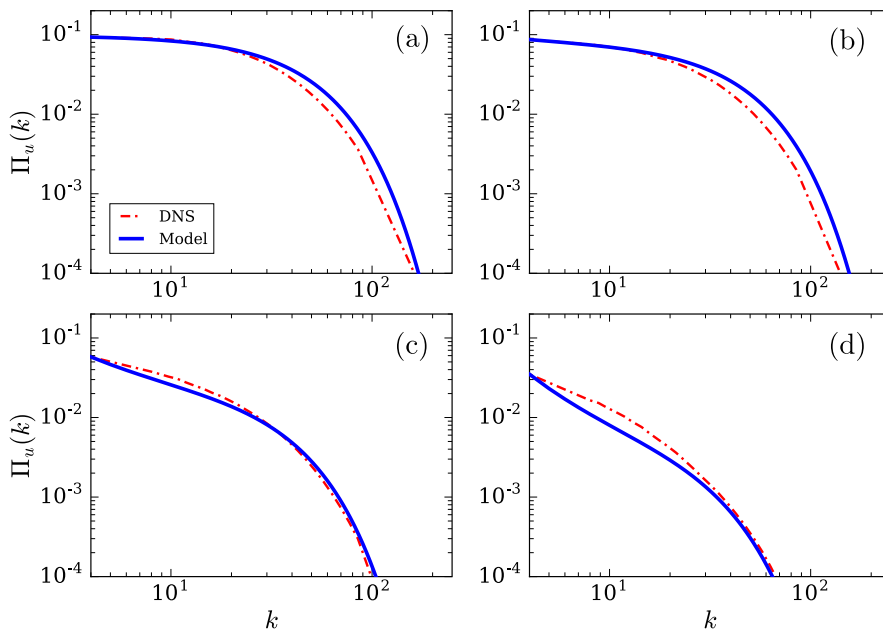


FIG. 5. For QS MHD turbulence, plots of the energy flux for (a)  $N = 0.0$ , (b)  $N = 0.1$ , (c)  $N = 0.5$ , and (d)  $N = 1.0$  reported by Ref. [28] (dot-dashed lines) and from the model predictions (solid lines).

#### IV. CONCLUSIONS

Modeling turbulent flows is a big challenge in science and engineering. In the present paper, we consider Ekman and quasi-static MHD turbulence; these flows exhibit steepening in the energy spectrum compared with their hydrodynamic counterpart due to additional dissipation arising from Ekman friction and Joule heating. We extend Pao's hypothesis for hydrodynamic turbulence to these flows and employ a variable energy flux formalism. This exercise yields energy spectra and fluxes for these flows in both inertial and dissipation range. We compare our model predictions with earlier experimental and numerical results and find them to be in good agreement with each other.

The success of our model encourages us to attempt a similar exercise for other turbulent flows. For large  $N$ , QS MHD turbulence becomes quasi-two-dimensional. Hence, for modeling such flows, it may be better to start with two-dimensional turbulence (similar to the model described in Sec. II). This exercise will be taken up in the future. Recently, Sharma *et al.* [45] employed Pao's hypothesis to model the energy spectrum of rapidly rotating turbulence. We envisage that Pao's hypothesis may be useful for modeling MHD turbulence, buoyancy-driven turbulence, etc.

#### ACKNOWLEDGMENTS

We thank Manohar Kumar Sharma, Roshan Samuel, Shashwat Bhattacharya, and Shadab Alam for useful discussions on Pao's hypothesis. This work was supported by Research Grant No. PLANEX/PHY/2015239 from the Indian Space Research Organization, India.

- 
- [1] A. N. Kolmogorov, Dissipation of energy in locally isotropic turbulence, Dokl. Acad. Nauk. SSSR **32**, 16 (1941).  
 [2] A. N. Kolmogorov, The local structure of turbulence in incompressible viscous fluid for very large Reynolds numbers, Dokl. Acad. Nauk. SSSR **30**, 301 (1941).

- [3] S. B. Pope, *Turbulent Flows* (Cambridge University Press, Cambridge, 2000).
- [4] M. Lesieur, *Turbulence in Fluids* (Springer-Verlag, Dordrecht, 2008).
- [5] U. Frisch, *Turbulence: The Legacy of A. N. Kolmogorov* (Cambridge University Press, Cambridge, 1995).
- [6] P. A. Davidson, *Turbulence: An Introduction for Scientists and Engineers* (Oxford University Press, Oxford, 2004).
- [7] P. A. Davidson, *Turbulence in Rotating, Stratified and Electrically Conducting Fluids* (Cambridge University Press, Cambridge, 2013).
- [8] A. S. Monin and A. M. Yaglom, *Statistical Fluid Mechanics: Mechanics of Turbulence* (Dover Publications, New York, 1973).
- [9] M. K. Verma, A. Kumar, and A. Pandey, Phenomenology of buoyancy-driven turbulence: Recent results, [New J. Phys.](#) **19**, 025012 (2017).
- [10] M. K. Verma, Anisotropy in quasi-static magnetohydrodynamic turbulence, [Rep. Prog. Phys.](#) **80**, 087001 (2017).
- [11] M. K. Verma, *Physics of Buoyant Flows: From Instabilities to Turbulence* (World Scientific, Singapore, 2018).
- [12] K. Nam, E. Ott, T. M. Antonsen, and P. N. Guzdar, Lagrangian Chaos and the Effect of Drag on the Enstrophy Cascade in Two-Dimensional Turbulence, [Phys. Rev. Lett.](#) **84**, 5134 (2000).
- [13] M. K. Verma, Variable enstrophy flux and energy spectrum in two-dimensional turbulence with Ekman friction, [Europhys. Lett.](#) **98**, 14003 (2012).
- [14] V. Pandey, P. Perlekar, and D. Mitra, Clustering and energy spectra in two-dimensional dusty gas turbulence, [Phys. Rev. E](#) **100**, 013114 (2019).
- [15] B. Knaepen and P. Moin, Large-eddy simulation of conductive flows at low magnetic Reynolds number, [Phys. Fluids](#) **16**, 1255 (2004).
- [16] J. Paret and P. Tabeling, Experimental Observation of the Two-Dimensional Inverse Energy Cascade, [Phys. Rev. Lett.](#) **79**, 4162 (1997).
- [17] M. Rivera, P. Vorobieff, and R. E. Ecke, Turbulence in Flowing Soap Films: Velocity, Vorticity, and Thickness Fields, [Phys. Rev. Lett.](#) **81**, 1417 (1998).
- [18] R. H. Kraichnan, Inertial ranges in two-dimensional turbulence, [Phys. Fluids](#) **10**, 1417 (1967).
- [19] A. Belmonte, W. I. Goldburg, H. Kellay, M. A. Rutgers, B. Martin, and X. L. Wu, Velocity fluctuations in a turbulent soap film: The third moment in two dimensions, [Phys. Fluids](#) **11**, 1196 (1999).
- [20] M. Rivera and X. L. Wu, External Dissipation in Driven Two-Dimensional Turbulence, [Phys. Rev. Lett.](#) **85**, 976 (2000).
- [21] G. Boffetta, A. Cenedese, S. Espa, and S. Musacchio, Effects of friction on 2D turbulence: An experimental study of the direct cascade, [Europhys. Lett.](#) **71**, 590 (2005).
- [22] H. Kellay and W. I. Goldburg, Two-dimensional turbulence: A review of some recent experiments, [Rep. Prog. Phys.](#) **65**, 845 (2002).
- [23] G. Boffetta and R. E. Ecke, Two-dimensional turbulence, [Annu. Rev. Fluid Mech.](#) **44**, 427 (2012).
- [24] G. Boffetta, A. Celani, S. Musacchio, and M. Vergassola, Intermittency in two-dimensional Ekman-Navier-Stokes turbulence, [Phys. Rev. E](#) **66**, 026304 (2002).
- [25] P. A. Davidson, *An Introduction to Magnetohydrodynamics*, 2nd ed. (Cambridge University Press, Cambridge, 2017).
- [26] R. J. Moreau, *Magnetohydrodynamics* (Springer, Berlin, 1990).
- [27] B. Knaepen and R. Moreau, Magnetohydrodynamic turbulence at low magnetic Reynolds number, [Annu. Rev. Fluid Mech.](#) **40**, 25 (2008).
- [28] M. K. Verma and K. S. Reddy, Modeling quasi-static magnetohydrodynamic turbulence with variable energy flux, [Phys. Fluids](#) **27**, 025114 (2015).
- [29] M. Hossain, Inverse energy cascades in three-dimensional turbulence, [Phys. Fluids B](#) **3**, 511 (1991).
- [30] T. Ishida, Small-scale anisotropy in magnetohydrodynamic turbulence under a strong uniform magnetic field, [Phys. Fluids](#) **19**, 075104 (2007).
- [31] A. VorobeV, O. Zikanov, P. A. Davidson, and B. Knaepen, Anisotropy of magnetohydrodynamic turbulence at low magnetic Reynolds number, [Phys. Fluids](#) **17**, 125105 (2005).

- [32] Y.-H. Pao, Structure of turbulent velocity and scalar fields at large wavenumbers, [Phys. Fluids](#) **8**, 1063 (1965).
- [33] M. K. Verma, A. Kumar, P. Kumar, S. Barman, A. G. Chatterjee, R. Samtaney, and R. Stepanov, Energy spectra and fluxes in dissipation range of turbulent and laminar flows, [Fluid Dyn.](#) **53**, 728 (2018).
- [34] G. Falkovich, Bottleneck phenomenon in developed turbulence, [Phys. Fluids](#) **6**, 1411 (1994).
- [35] M. K. Verma and D. A. Donzis, Energy transfer and bottleneck effect in turbulence, [J. Phys. A: Math. Theor.](#) **40**, 4401 (2007).
- [36] C. Küchler, G. Bewley, and E. Bodenschatz, Experimental study of the bottleneck in fully developed turbulence, [J. Stat. Phys.](#) **175**, 617 (2019).
- [37] D. Biskamp, E. Schwarz, and A. Celani, Nonlocal Bottleneck Effect in Two-Dimensional Turbulence, [Phys. Rev. Lett.](#) **81**, 4855 (1998).
- [38] A. Alemany, R. Moreau, and U. Frisch, Influence of an external magnetic field on homogeneous MHD turbulence, [J. Mec.](#) **18**, 277 (1979).
- [39] S. Eckert, G. Gerbeth, W. Witke, and H. Langenbrunner, MHD turbulence measurements in a sodium channel flow exposed to a transverse magnetic field, [Int. J. Heat Fluid Flow](#) **22**, 358 (2001).
- [40] K. S. Reddy, R. Kumar, and M. K. Verma, Anisotropic energy transfers in quasi-static magnetohydrodynamic turbulence, [Phys. Plasmas](#) **21**, 102310 (2014).
- [41] O. Zikanov and A. Thess, Direct numerical simulation of forced MHD turbulence at low magnetic Reynolds number, [J. Fluid Mech.](#) **358**, 299 (1998).
- [42] K. S. Reddy and M. K. Verma, Strong anisotropy in quasi-static magnetohydrodynamic turbulence for high interaction parameters, [Phys. Fluids](#) **26**, 025109 (2014).
- [43] D. A. Donzis and K. R. Sreenivasan, The bottleneck effect and the Kolmogorov constant in isotropic turbulence, [J. Fluid Mech.](#) **657**, 171 (2010).
- [44] T. Ishihara, K. Morishita, M. Yokokawa, A. Uno, and Y. Kaneda, Energy spectrum in high-resolution direct numerical simulations of turbulence, [Phys. Rev. Fluids](#) **1**, 082403(R) (2016).
- [45] M. K. Sharma, A. Kumar, M. K. Verma, and S. Chakraborty, Statistical features of rapidly rotating decaying turbulence: Enstrophy and energy spectra and coherent structures, [Phys. Fluids](#) **30**, 045103 (2018).